International Journal of Engineering & Applied Sciences (IJEAS)
Vol.3, Issue 1(2011)1-14

ESTIMATION OF DRAWING FORCE IN DRAWING OF TWISTED SQUARE SECTION ROD FROM ROUND BAR

Haghighat, H., Allahveysi, S.B. and Akhavan, A.
[1]Mechanical Engineering Department, Razi University, Kermanshah, Iran

Received Date: 06 August 2010; Accepted Date: 18 September 2010

Abstract

Drawing of twisted square section rod from round bar has been studied in this paper. The drawing force was determined via an upper bound solution based on an equivalent axisymmetric curved die. By determining the profile of the equivalent curved die, a velocity field which considered the twist of material inside the die was presented. Then, internal, shearing and frictional powers were calculated and drawing force was estimated by equating the summation of these powers with required external power. For assuring of the results of analysis, various experiments were performed for St 33 bars in diameters of 10, 8 and 6 mm to twisted square section rods with sides of 8, 6 and 5 mm, respectively. Comparison of the experimental and theoretical drawing forces showed an acceptable agreement.

Keywords: Twisted square section rod, Drawing force, Experiment

Nomenclature

F_d drawing force
J^* external power of deformation
L length of die
m friction factor $(0 \le m \le 1)$
R instantaneous radius at outer-surface of the material inside equivalent die
R_f equivalent radius of square rod
R_o radius of circular bar
r, θ, z cylindrical coordinates
r_f radial position of the S3 surface of velocity discontinuity
r_o radial position of the S1 surface of velocity discontinuity
S1 first surface of velocity discontinuity, separating the incoming bar from the deformation zone
S2 second surface of velocity discontinuity, separating the deformation zone from the final product
U_r, U_θ, U_ϕ radial, angular and rotational components of velocity
u_f velocity of the rod at the exit of the die
u_o velocity of the bar at the entrance of the die
$\dot{W}_i$ internal power of deformation
$\dot{W}_{S1}$ shear power losses along S1 surface of velocity discontinuity
$\dot{W}_{S2}$ shear power losses along S2 surface of velocity discontinuity

$\dot{W}_f$ friction power losses along the die-material interface

α semi-die angle of equivalent die

β arbitrary angle

ΔU_1 tangential velocity difference along the S1 surface of velocity discontinuity

ΔU_2 tangential velocity difference along the S2 surface of velocity discontinuity

ΔU_f tangential velocity difference along the die surface

$\dot{\varepsilon}_{rr}$ normal strain rate component in the radial direction

$\dot{\varepsilon}_{\theta\theta}$ normal strain rate component in the angular direction

$\dot{\varepsilon}_{\phi\phi}$ normal strain rate component in the rotational direction

$\dot{\varepsilon}_{r\theta}, \dot{\varepsilon}_{r\phi}, \dot{\varepsilon}_{\theta\phi}$ shear strain rate components

σ_0 average of yield stress of the workpiece material

ω_d angular velocity of the die

ψ angular position of the equivalent die profile

1. Introduction

Twisted square section rods are used in lid of channels, at the bottom of workshops and metallic stairs in which personnel slippage on them is exist. Moreover, they are used in manufacturing twisted nails with square cross section. Drawing through the rotating dies is a simple method for manufacturing twisted rods. In this process, like another metal forming processes, notification of drawing force is very important. Estimating the required drawing force is essential for designing the die and selecting the machine with enough capacity. The process of wire drawing through smooth conical dies was first analyzed by Sachs [1], for rigid plastic materials. The basic assumption of his analysis is that the plane sections remain plane during the deformation. Later several authors extended Sachs' analysis to include the effects of other variables such as friction, work hardening and strain rate [2, 3]. Siebel [4] took into account both the die friction and the redundant deformation along with the homogeneous deformation. The experiments conducted by Wistreich [5], with split dies, established that for any drawing operation the drawing stress is minimum at a particular value of the die angle called the optimum angle. Subsequently Avitzur survived the characteristics of metal flow in drawing process through converging dies [6]. Then he verified the effects of work hardening in plastic flow [7]. Afterwards he analyzed the drawing process by assuming a spherical velocity field in the zone of plastic deformation [8]. Besides predicting the optimum die angle, his analysis shows a gradual transition from the drawing to the shaving process as the die angle is increased. All the theories developed so far concern the drawing of circular wires through semi conical dies. Upper bound approach for drawing of circular wires to square shape was first utilized by Basily [9]. He calculated drawing force by meshing the deformation zone and defining a spherical velocity field for each node and finally solved the whole geometry of deformation by use of a computer program. He also presented some techniques for the measurement of mean coefficient of friction in the direct drawing of section rod from round bar [10, 11]. Gunaserka and Hoshino [12] accomplished the upper bound solution for analyzing drawing and extrusion of circular rods to square section bars through converging dies which were formed by straight lines. Su [13], performed experiments for

measuring drawing load in drawing processes and surveyed final product. Wang [14], presented semi analytical finite element method. He also simulated and analyzed drawing process of round bar to section rod by means of finite element software [15]. Knap [16], described the process and the circumstance of deformation of material in process of drawing of circular wire to twisted square section rod. He also surveyed the experimental affection of the semi die angle. Ma and Barnett [17, 18], analyzed the process of forward extrusion thorough rotating dies, theoretically and experimentally. They provided required torque for rotating the die from an external source, and they also supposed that the angular velocity of the material inside the die, changes with a power relation in relate to radius of each position in proportion to apex of virtual conic of the die. After that, they inspected the effect of slippage factor and semi die angle in extrusion pressure and finally determined the optimum die angle.

In this study, upper bound approach, based on equivalent die, was utilized for estimating the required force in drawing a circular bar to a twisted square section rod. Spherical velocity field which includes twisting the material in the region of plastic deformation was suggested. Some drawing experiments were performed and drawing forces were measured. Then, the results of upper bound approach were compared with experimental drawing forces.

2. Description of the process

The working surface of the die has a shape which allows the round bar deform into square rod and also twist it, simultaneously. In order to obtain gradual shaping of the cross section during the decrease of its area, the working surface of the die is inclined under a constant angle to the die axis. Due to the existence of the helix angle inside the die, die starts to rotate when the drawing process starts. Shaping the twisted rod starts at the corners of the cross section. As the metal flows through the die, the contribution of the straight lines increases and the contribution of the arcs decrease. This process is shown in Fig. 1. Because of the complexity of the metal flow inside the die, analysing the real process is complicated. In this study, the idea is to analyze the equivalent axisymmetric process instead of complicated real process. In equivalent process, in each position on the die axis, perpendicular cross sections on the actual die and the equivalent die have the same area. The profile of equivalent axisymmetric curved die is shown in Fig. 2. In this figure, circular bar with initial radius R_o is drawn through the axisymmetric curved die with semi-die angle α and its radius is reduced to R_f, where α is the angle between the line that goes through the point where the die starts touching the bar, and the exit point of the die and the die axis of symmetry.

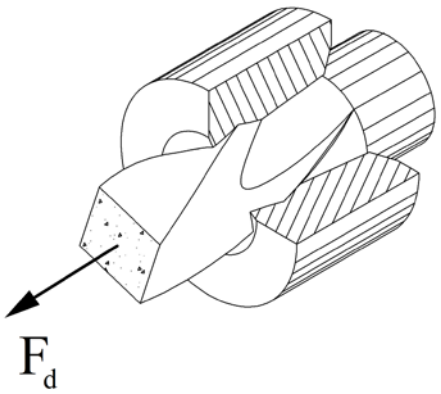

Fig. 1. Drawing process of a circular round bar to a twisted square section rod

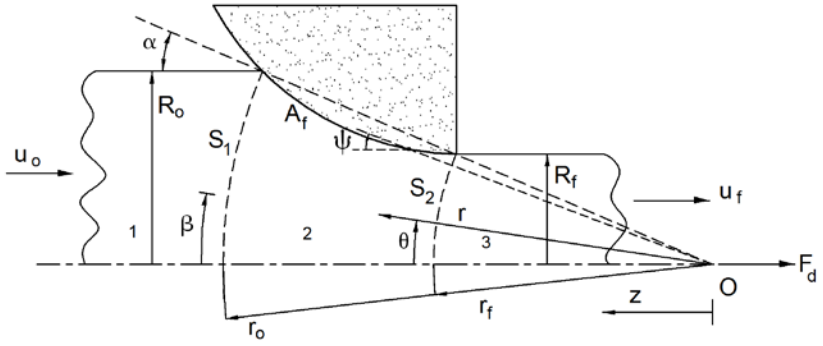

Fig. 2. Equivalent axisymmetric curved die, geometric parameters and its deformation zones

3. Upper bound analysis based on the equivalent axisymmetric curved die

The general equation to calculate the external power of deformation for a material with flow stress σ_0 in an upper bound model is [19]

$$J^* = \frac{2}{\sqrt{3}}\sigma_0 \int_V \sqrt{\frac{1}{2}\dot{\varepsilon}_{ij}\dot{\varepsilon}_{ij}}\, dV + \frac{\sigma_0}{\sqrt{3}}\int_{As} |\Delta U| dS + m \frac{\sigma_0}{\sqrt{3}}\int_{Af} |\Delta U| dS \qquad (1)$$

where the first term of Eq. (1) is the internal power of deformation in the whole material volume, the second term is wasted shearing power, the third term is wasted frictional power, $\dot{\varepsilon}_{ij}$ are terms of strain rates, $|\Delta U|$ is velocity discontinuity, dS is surface element and m is shearing friction factor.

The first step in modeling and analysing a metal forming process by use of upper bound approach is to select a suitable velocity field for the material which is deforming plastically. Fig. 2 shows a schematic diagram for the spherical coordinate system and the three velocity zones used in upper bound analysis. A spherical coordinate system is used to describe the position of the two surfaces of velocity discontinuity as well as the velocity in zones 1 to 3. The spherical coordinate system (r, θ, ϕ) is centered on the convergence point of the equivalent axisymmetric curved die. This point, as shown in Fig. 2, is defined by the intersection of the axis of symmetry with a line that goes through the point where the die starts touching the bar and the outlet point of the die. In zone 1, the incoming material is assumed to flow horizontally as a rigid body with a velocity u_o. In zone 3, the drawn material is assumed to flow horizontally as a rigid body with a velocity u_f. Zone 2 is the deformation region, where the velocity is fairly complex. Zone 1 is separated from zone 2 by a surface of velocity discontinuity, S1. Zone 3 is separated from zone 2 by a surface of velocity discontinuity, S2. The mathematical equations for radial positions of these two surfaces of velocity discontinuity are given by $r_f = R_f / \sin\alpha$ and $r_o = R_o / \sin\alpha$ for surfaces S1 and S2, respectively.

Zone 1: In this zone, material enters the die as a rigid body and velocity components are

$$U_r = -u_0 \cos\theta, \quad U_\theta = u_0 \sin\theta, \quad U_\phi = 0 \qquad (2)$$

where u_o is the speed of the bar in the entrance of the die and it is

$$u_o = \left(\frac{R_f}{R_o}\right)^2 u_f \tag{3}$$

Zone 2: The base radial velocity within this zone U_r can be obtained by assuming the volume flow balance. In Fig. 2, the volume flow of the material across the surface S1 at the point (r_0, β, ϕ) in the radial direction is

$$dQ = -u_0 \cos\beta (r_0 d\beta)(r_0 \sin\beta) d\phi \tag{4}$$

The volume flow of the material in the radial direction at the point (r, θ, ϕ) in the deformation region (see Fig. 2) is

$$dQ = U_r (r d\theta)(r \sin\theta) d\phi \tag{5}$$

By equating Eqs. (4) and (5), the base radial velocity component in zone 2 is found to be

$$U_r = -u_0 (\frac{r_0}{r})^2 \frac{\sin\beta}{\sin\theta} \cos\beta \frac{d\beta}{d\theta} \tag{6}$$

If assuming the proportional distance in a cylindrical sense from the centreline [20], then it yields

$$\frac{\sin\beta}{\sin\theta} = \frac{\sin\alpha}{\sin\psi} \tag{7}$$

where ψ is the angular position of a point on the equivalent die curve at radial position r. By differentiating Eq. (7), it yields

$$\cos\beta \frac{d\beta}{d\theta} = \sin\alpha \frac{\cos\theta}{\sin\psi} \tag{8}$$

By Substituting Eq. (8) in Eq. (6), the radial velocity component is obtained as

$$U_r = -u_o \left(\frac{r_o}{r}\right)^2 \frac{\sin^2\alpha \cos\theta}{\sin^2\psi} \tag{9}$$

The full velocity field for the metal flow in the deformation zone 2 is obtained by invoking the volume constancy. The volume constancy in spherical coordinates is defined as

$$\dot{\varepsilon}_{rr} + \dot{\varepsilon}_{\theta\theta} + \dot{\varepsilon}_{zz} = 0 \tag{10}$$

where $\dot{\varepsilon}_{ii}$ is the normal strain rate component in the i-direction. The strain rates in spherical coordinates are defined as

$$\dot{\varepsilon}_{rr} = \frac{\partial U_r}{\partial r}$$

$$\dot{\varepsilon}_{\theta\theta} = \frac{1}{r}\frac{\partial U_\theta}{\partial \theta} + \frac{U_r}{r}$$

$$\dot{\varepsilon}_{\phi\phi} = \frac{1}{r\sin\theta}\frac{\partial U_\phi}{\partial \phi} + \frac{U_r}{r} + \frac{U_\theta}{r}\cot\theta$$

$$\dot{\varepsilon}_{r\theta} = \frac{1}{2}\left(\frac{\partial U_\theta}{\partial r} - \frac{U_\theta}{r} + \frac{1}{r}\frac{\partial U_r}{\partial \theta}\right) \tag{11}$$

$$\dot{\varepsilon}_{\theta\phi} = \frac{1}{2}\left(\frac{1}{r\sin\theta}\frac{\partial U_\theta}{\partial \phi} + \frac{1}{r}\frac{\partial U_\phi}{\partial \theta} - \frac{\cot\theta}{r}U_\phi\right)$$

$$\dot{\varepsilon}_{\phi r} = \frac{1}{2}\left(\frac{\partial U_\phi}{\partial r} - \frac{U_\phi}{r} + \frac{1}{r\sin\theta}\frac{\partial U_r}{\partial \phi}\right)$$

where $\dot{\varepsilon}_{ii}$ (with $i = j$) is a shear strain rate component. With assumption of the rotational motion of the material in the deformation zone 2, the rotational component of velocity for a point in this zone can be given by

$$U_\phi = r\omega_d \sin\theta \tag{12}$$

The angular component of velocity field is obtained by placing U_r and U_ϕ, Eqs. (7) and (12) into Eq. (10) and solving for U_θ, and apply the boundary condition along the centerline, then

$$U_\theta = -u_o \frac{r_o^2}{r}\frac{\dfrac{\partial \psi}{\partial r}\sin^2\alpha\sin\theta}{\sin^2\psi\tan\psi} \tag{13}$$

where the angular velocity of the die ω_d depends on drawing speed u_f and helix angle of die λ, as

$$\omega_d = \frac{u_f}{R_f \tan\lambda} \tag{14}$$

If the helix angle of the die is $\lambda = 90^\circ$, then angular velocity of the die will be equal to zero and consequently square section exits from the die without twisting.

Zone 3: In this zone, material leaves the die as a rigid body and the velocity field is

$$U_r = -u_f \cos\theta, \quad U_\theta = u_f \sin\theta, \quad U_\phi = 0 \tag{15}$$

The strain rate tensor for zone 2 can be obtained by using Eq. (11).

$$\dot{\varepsilon}_{rr} = 2u_o\left(\frac{r_o}{r}\right)^2 \frac{\sin^2\alpha\cos\theta}{\sin^2\psi}\left(\frac{1}{r} + \frac{\dfrac{\partial\psi}{\partial r}}{\tan\psi}\right)$$

$$\dot{\varepsilon}_{\theta\theta} = -u_o\left(\frac{r_o}{r}\right)^2 \frac{\sin^2\alpha\cos\theta}{\sin^2\psi}\left(\frac{1}{r} + \frac{\dfrac{\partial\psi}{\partial r}}{\tan\psi}\right)$$

$$\dot{\varepsilon}_{\phi\phi} = -u_o\left(\frac{r_o}{r}\right)^2 \frac{\sin^2\alpha\cos\theta}{\sin^2\psi}\left(\frac{1}{r} + \frac{\dfrac{\partial\psi}{\partial r}}{\tan\psi}\right) \tag{16}$$

$$\dot{\varepsilon}_{r\theta} = -\frac{u_o}{2}\left(\frac{r_o}{r}\right)^2 \frac{\sin^2\alpha\sin\theta}{\tan\psi\sin^2\psi}\left(2\frac{\partial\psi}{\partial r} - r\frac{\partial^2\psi}{\partial r^2} + \frac{2r\left(\dfrac{\partial\psi}{\partial r}\right)^2}{\tan\psi} + r\left(\frac{\partial\psi}{\partial r}\right)^2(1+\tan^2\psi) + \frac{\tan\psi}{r}\right)$$

$$\dot{\varepsilon}_{\theta\phi} = \dot{\varepsilon}_{\phi r} = 0$$

with the strain rate tensor and the velocity field, the standard upper bound method can be implemented. This method involves calculating the internal power of deformation over the deformation zone volume, the shear power losses over two surfaces of velocity discontinuity (shear surfaces), and the frictional power losses between the workpiece and the tooling.
The equation for calculating the internal power of deformation in zone 2 that is surrounded by two velocity discontinuity surfaces of S_1 and S_2 as well as the die surface, is calculated as

$$\dot{W}_i = 2\pi\frac{2\sigma_\circ}{\sqrt{3}}\int_{r_f}^{r_o}\int_0^{\psi}\sqrt{\frac{1}{2}\dot{\varepsilon}^2{}_{rr} + \frac{1}{2}\dot{\varepsilon}^2{}_{\theta\theta} + \frac{1}{2}\dot{\varepsilon}^2{}_{\phi\phi} + \dot{\varepsilon}^2{}_{r\theta}}\; r^2\sin\theta\, d\theta\, dr \tag{17}$$

Equation for the power losses along the shear surface of velocity discontinuity S_1 can be given by

$$\dot{W}_{S_1} = 2\pi\frac{\sigma_\circ}{\sqrt{3}}\int_0^{\alpha=\psi(r_o)}\left|\Delta U_1\right| r_o^2\sin\theta\, d\theta \tag{18}$$

With

$$\Delta U_1 = \left[\left(U_o\sin\theta + \frac{u_o r_o \left.\dfrac{\partial\psi}{\partial r}\right|_{r=r_o}\sin\theta}{\tan\alpha}\right)^2 + (r_o\omega_d\sin\theta)^2\right]^{\frac{1}{2}} \tag{19}$$

The shear power losses along the surface of velocity discontinuity S_2 are calculated as

$$\dot{W}_{S_2} = 2\pi \frac{\sigma_\circ}{\sqrt{3}} \int_0^{\alpha=\psi(r_f)} |\Delta U_2| r_f^2 \sin\theta \, d\theta \tag{20}$$

With

$$\Delta U_2 = [(u_f \sin\theta + \frac{u_f r_f \left.\frac{\partial \psi}{\partial r}\right|_{r=r_f}}{\tan\alpha} \sin\theta)^2 + (r_f \omega_d \sin\theta)^2]^{\frac{1}{2}} \tag{21}$$

Equation for the friction power losses along the die surface with a constant friction factor is

$$\dot{W}_f = 2\pi \frac{m\sigma_\circ}{\sqrt{3}} \frac{1}{\sin\lambda} \int_{r_f}^{r_o} |\Delta U_f| r \sin\psi \, d\psi \tag{22}$$

With

$$\Delta U_f = \left[U_r \cos\xi + U_\theta \sin\xi\right]\big|_{\theta=\psi} \tag{23}$$

$$\cos\xi = \frac{r\frac{\partial\psi}{\partial r}}{\sqrt{\left(r\frac{\partial\psi}{\partial r}\right)^2 + 1}}, \sin\xi = \frac{1}{\sqrt{\left(r\frac{\partial\psi}{\partial r}\right)^2 + 1}} \tag{24}$$

where the constant friction factor, m, can take on values from 0 to 1. The total externally supplied power J^* is

$$J^* = F_d u_f \tag{25}$$

By the upper bound theorem, this power is less than or equal to the sum of the power terms in Eqs. (17), (18), (20) and (22). If one assumes equality then

$$J^* = \dot{W}_i + \dot{W}_{S_1} + \dot{W}_{S_2} + \dot{W}_f \tag{26}$$

Finally, drawing force was calculated through dividing J^* by drawing speed u_f. In the present investigation, the integrals that are presented in the power terms are evaluated by numerical integration.

4. Experiments and discussion

4.1 Experimental conditions and geometry of the drawing die

In order to verify the theoretical results, experiments using three real rods used as industrial rods have been performed. The material for the experiments was St 33 and the same as material used for theoretical study. The chemical compositions of St 33 are shown in Table 1. The stress–strain curve of the material was obtained using tensile test and it is shown in Fig. 3. The apparatus for the experiments is shown in Fig. 4. First, the drawing die is inserted and fixed in upper tool set. Then, the material is inserted in the drawing die and the given material is drawn by the lower jaw. The drawing speed was 1 mm/s. The initial round bars were 6 mm (Case I), 8 mm (Case II) and 10 mm (Case III) in diameters. They are drawn to twisted square section rods with sides of 5, 6 and 8 mm, respectively. The material of drawing dies were tungsten carbide with the helix angles of 83°, 80° and 77° and their lengths were 7, 7 and 10 mm, respectively. Drawing process was operated without lubricant. Fig. 5 shows produced rods in the experiments.

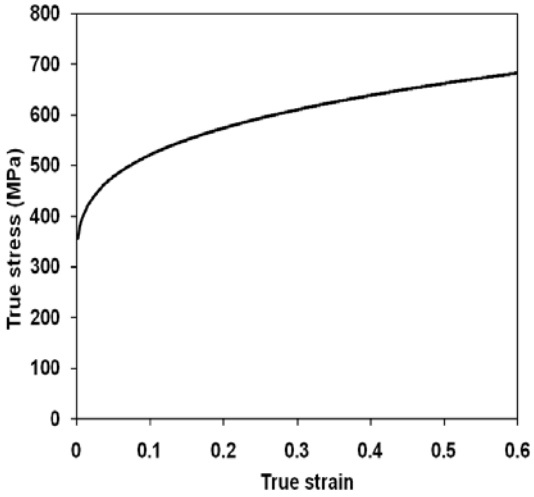

Fig. 3. Stress–strain curve of St 33

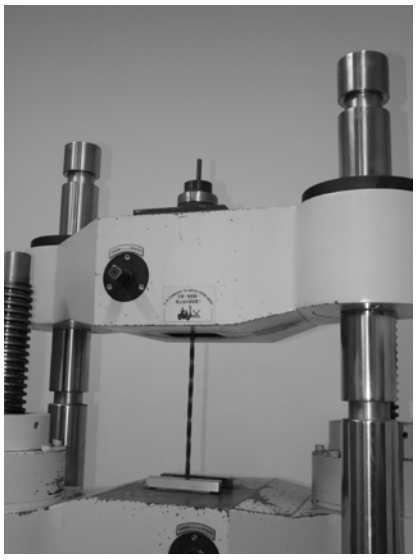
Fig. 4. Experimental apparatus for the shaped drawing process

Fig. 5. Drawn rods

4.2 Results and discussion

The results of the experiments, measured drawing forces, for these three cases are shown in Fig 6. The results of theoretical and experimental data for drawing forces are compared in Table 1. This table shows that the error percentage for Cases I, II and III are 15%, 17% and 20%, respectively.

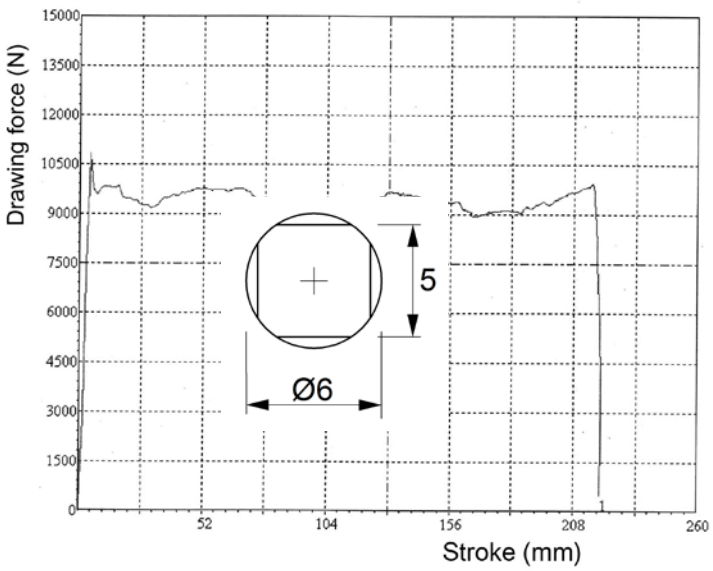

Fig. 6. Experimental drawing forces for three cases (a. Case I)

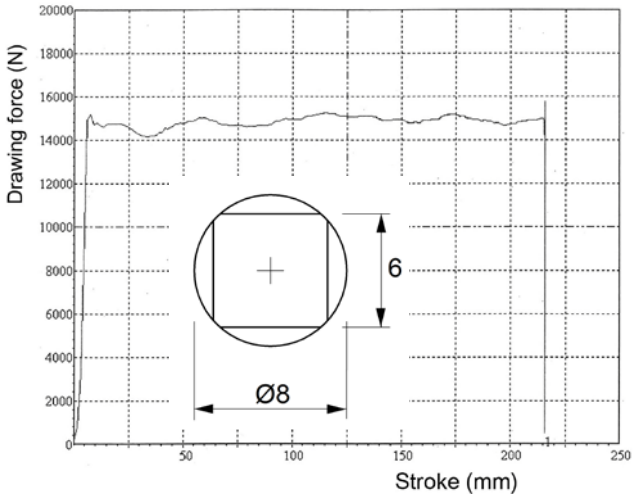

Fig. 6. Experimental drawing forces for three cases (b. Case II)

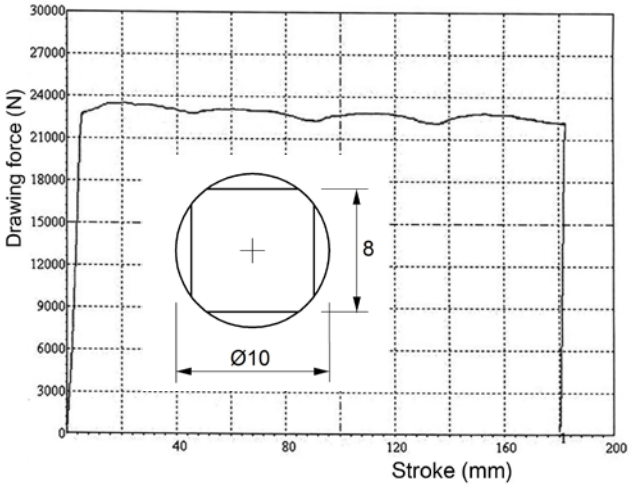

Fig. 6. Experimental drawing forces for three cases (c. Case III)

Table 1. Analytical and theoretical drawing forces for three cases.

Case No.	**Analytical drawing force (KN)**	**Experimental drawing force (KN)**
I	10.96	9.5
II	17.60	15.5
III	30.19	24

There are two reasons for this matter. The first one is because of using the equivalent die and the second is due to the nature of upper bound method in which the force is over estimated.The relation of drawing force and semi-die angle α for different helix angles is illustrated in Fig. 7. As it is shown, the optimum die angle decreases when helix angle increases.

The effect of semi-die angle α on drawing force is shown in Fig. 8 for different values of *m*. As it is expected, for a given value of *m*, there is an optimum die angle in which the power is minimized. It is also observed that the optimum die angle increases when shearing friction factor increases.

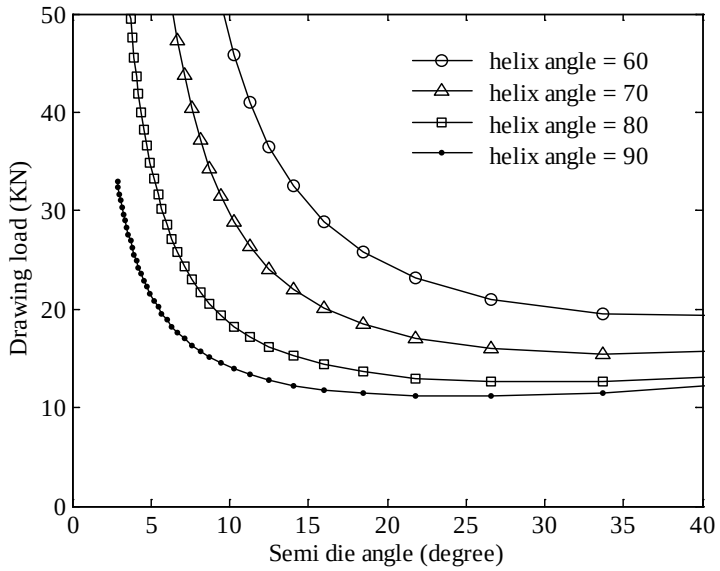

Fig. 7. Effect of helix angle of the die on the optimum semi-die angle

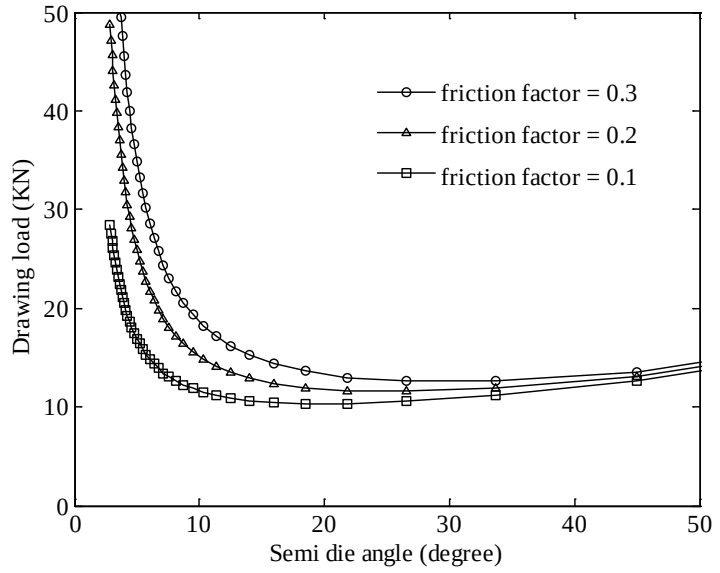

Fig. 8. Effect of friction factor on the optimum semi-die angle

5. Conclusions

In the process of drawing of twisted square section rod from circular bar, the drawing force was estimated based on an equivalent axisymmetric curved die by utilizing the upper bound approach. An admissible velocity field which considered the twist of material inside the die

was assumed. In order to verify the possibility of the application of theoretical results by using the upper bound method, experiments of the shaped drawing for three real industrial products were performed and the results were in acceptable agreement with theoretical results. By increasing the helix angle of die, the optimum semi-die angle decreases. Optimum die angle increases when shear friction factor increases.

References

[1] Sachs, G., On the theory of the tensile test, *Zeitschrift fuer Angewandte Mathematik und Mechanik*, 7, 235–6, 1927 (in German).
[2] Korber, F., Eichinger, A., *Metteilungen aus dem Kaiser-Wilhelm Institute fur Eisenforchung*, 66, A-193, 1940.
[3] Sachs, G., Lubahn, J.D., and Tracy, D.O., Drawing thin walled tubing with a moving mandrel and die, *J. Appl. Mech. Trans. ASME*, 11, 199-210, 1944.
[4] Siebel, E., Der derzeitiger stand der erkentnisse uber die, mechanischen beim drahtziehen. *Stahl und Eisen*, 171-180, 1947.
[5] Wistreich, J.G., Investigation of the mechanics of wire drawing, Proc. Inst. Mech. Engrs. (London), l69, 654-665, 1955.
[6] Avitzur B., Flow Characteristics through conical converging dies, *J. Eng. Ind. Trans. ASME Series B*, 88, 410-420, 1966.
[7] Avitzur. B., Strain-hardening and strain-rate effects in plastic flow through conical converging dies, *J. Eng. Ind. Trans. ASME*, 89, 556-562, 1997.
[8] Avitzur, B., *Metal Forming: Processes and Analysis*, McGraw-Hill, New York, 1968
[9] Basily, B.B., Sansome, D.H., Some theoretical consideration for the direct drawing of section rod from round bar, *Int. J. of Mech. Sci.*, 18, 201-208, 1976.
[10] Basily, B.B., Sansome, D.H., Determination of the mean coefficient of friction in the direct drawing of section rods, 17th International Machinery Tool Designs and Research Conference (MTDR), 475-481, 1976.
[11] Basily, B.B., A new experimental technique for the measurement of mean coefficient of friction in the direct drawing of section rod from round bar, 24th International Machinery Tool Designs and Research Conference (MTDR), 85-88, 1983.
[12] Gunasekera, J.S., Hoshino, S., Analysis of extrusion or drawing of polygonal sections through straightly converging dies, *J. Eng. Ind. Trans ASME*, 104, 38–45, 1982.
[13] Su, Z.Y., Direct cold drawing of section rods from round bars through a single plum-shaped die, Technical Report, Steel Cold Drawing Company, Wenan County, Hebei Province, PR China, 1988.
[14] Wang, K.L., Design and analysis of direct cold drawing of section rods using semi-analytical finite element method, *Trans. NAMRI/SME XXVII*, 1-6, 1999.
[15] Wang, K.L., Argyropoulos, V., Design and analysis of direct cold drawing of section rods through a single die, *J. of Mater. Process. Technol.*,166, 345–358, 2005.
[16] Knap, F., Drawing of square twisted wire, *J. of Mater. Process. Technol.*, 60,167-170, 1996.
[17] Ma, X., Barnett, M.R., and Kim, Y.H., Forward extrusion through steadily rotating conical dies. Part II: theoretical analysis. *Int. J. of Mech. Sci*., 46, 465–489, 2004.
[18] Ma, X., Barnett, M.R., and Kim, Y.H., Forward extrusion through steadily rotating conical dies. Part I: experiments. *Int. J. of Mech. Sci*., 46, 449– 464, 2004.
[19] Prager, W., Hodge, P.G., *Theory of perfectly plastic solids*, John Wiley and Sons Inc. New York, 1951.

[20] Gordon, W.A., Van Tyne, C.J., and Moon, Y.H., Axisymmetric Extrusion through Adaptable Dies—Part 1: Flexible Velocity Fields and Power Terms, *Int. J. Mech. Sci.*, 49, 86–95, 2007.